

# Wind Tunnel Test on Generic Agusta-Bell 206B Helicopter Tail Rotor Blades

Firdaus<sup>a</sup>, Jaswar Koto<sup>a,b,\*</sup>, I.S. Ishak<sup>a</sup> and M.S. Ammoo<sup>a</sup>

<sup>a</sup>Department of Aeronautical, Automotive and Ocean Engineering, Faculty of Mechanical Engineering, Universiti Teknologi Malaysia

<sup>b</sup>Ocean and Aerospace Research Institute, Indonesia

\*Corresponding author: [jaswar@mail.fkm.utm.my](mailto:jaswar@mail.fkm.utm.my) and [jaswar.koto@gmail.com](mailto:jaswar.koto@gmail.com)

## Paper History

Received: 16-February-2015

Received in revised form: 22-February-2015

Accepted: 27-February-2015

CFD Computational Fluid Dynamic  
RPM Revolutions per Minute

## ABSTRACT

A low speed wind tunnel test was conducted for a full-scaled generic model of Agusta-Bell 206B helicopter tail rotor blades in the Universiti Teknologi Malaysia-Low Speed Tunnel (UTM-LST). The purpose of this paper is to conduct the experimental research for gaining information on general aerodynamics and performance characteristics of tail rotor blades. The lift and drag coefficients are examined in order to explore aerodynamic characteristics of the tail rotor blades. The present results may be useful to understand general aerodynamic characteristics and will be used in validation of the Quasi-Continuous Method (QCM) in the future.

**KEY WORDS:** *Wind Tunnel Test; Helicopter Tail Rotor Blades; Quasi Continuous Method.*

## NOMENCLATURE

VLM Vortex Lattice Method  
MFM Mode Function Method  
QCM Quasi Continuous Method  
SSPM Simple Surface Panel Method

## 1.0 INTRODUCTION

The propeller blade is the device that mainly used as propulsive for marine vehicles, airplanes and rotorcraft. As it is a crucial part, it has to be designed to meet power requirement at the indicated speed with optimum efficiency. Now days, with growing demands for of higher speed and greater power, the propeller is becoming increasingly larger in size and its geometry shape become more complicated. Due this complicated geometry, the propeller should be optimally designed for increased propulsion efficiency.

To predict the steady and unsteady propeller characteristics, many numerical models and propeller theories were proposed. One of them and will be used in this study is based on lifting surface theory. The lifting surface theory also plays as important role in the hydrodynamic analysis of marine propellers. The theory has been developed for a long time in the field of aeronautics. While almost all of the applications of the theory are to wings of airplanes, there is an old application to screw propellers (Kondo, 1942).

A number of methods based on lifting surface theory to estimate the propeller characteristics have been published. They can be classified into two groups. One group is based on the continuous loading method such as Mode Function Method (MFM) and the other the discrete loading method such as Vortex

Lattice Method (VLM). Due to the complexity in numerical calculation using MFM, its application to unconventional propellers is not easy. VLM, however, also has some room to be improved; in the neighborhood of leading edge, the vortex strength predicted by VLM is always lower compared with analytical solutions. Owing to the discrete and concentrated loading distribution, pressure distribution is not estimated straightforwardly. Leading edge suction force is not estimated straightforwardly either. A large number of elements are necessary to get converged solutions (Naoto Nakamura, 1985).

Taking the above circumstances into consideration, a numerical method to estimate aerodynamics characteristics of helicopter tail propeller based on Quasi-Continuous Method (QCM) will be developed. QCM has both advantages of continuous loading method and discrete loading method; loading distribution is assumed to be continuous in chord-wise direction and stepwise constant in span-wise direction. Simplicity and flexibility of the discrete loading method are also retained.

To validate this method, experimental procedure has been proposed with used the full scaled generic model tail rotor blades of Agusta- Bell 206B helicopter that was conducted in the UniversitiTeknologi Malaysia- Low Speed Tunnel (UTM-LST). Present data show the aerodynamic characteristics, lift coefficient and drag coefficient of the blade. And the sample data in time series at the angle of attack and speed selected will also present.

## 2.0 EXPERIMENTAL ARRANGEMENT

### 2.1 Wind Tunnel

The test was conducted in the UniversitiTeknologi Malaysia- Low Speed Tunnel (UTM-LST). The layout of wind tunnel aerodynamic circuit and indicates the important components within the wind tunnel circuit are illustrated in Figure 1.

The UTM-LST is a pressurized, closed-circuit, continuous-flow wind tunnel with an operating pressure from approximately 0.10 to 4 atmospheres. The test section size is 2.0 m wide x 1.5 m height x 5.5 m length. The wind tunnel has an excellent flow quality (flow uniformity < 0.15%, temperature uniformity < 0.2%, flow angularity uniformity < 0.15%, turbulence < 0.06%) that was mentioned in the AIAA paper (Elfstrom GM, 2007). And it is capable of delivering maximum airspeed of 80 m/s (160 knots or 288 km/hr) inside the test section (Alias Mohd Noor, 2013).

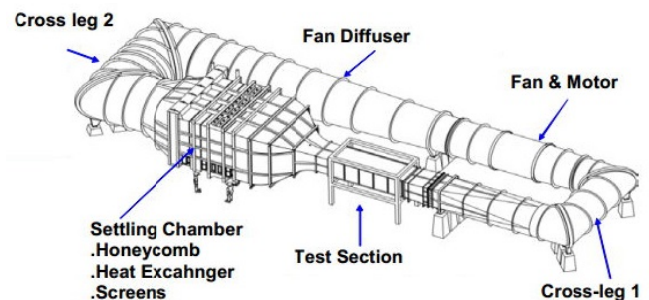


Figure 1: Wind tunnel components.

### 2.2 Tail Rotor Blade Model

Figure 2 shows the blades from the generic model of the tail rotor blades from Agusta-Bell 206B helicopter, with an actual scale will be used in this experiment. The blade was 720mm overall length and has 134mm length of the chord.

The airfoil profile of the blade is near similar to NACA 0012 series, with maximum thickness 12% at 33% chord as shown in Figure 3.

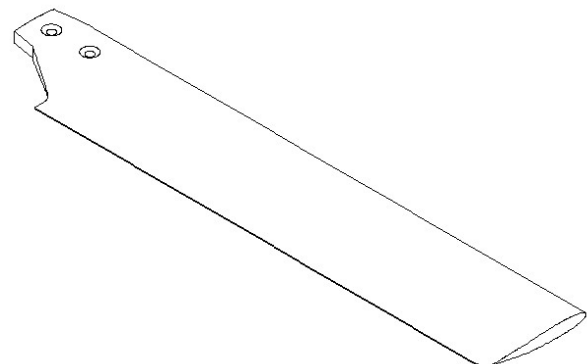


Figure 2: Used Bell B206 tail rotor blade

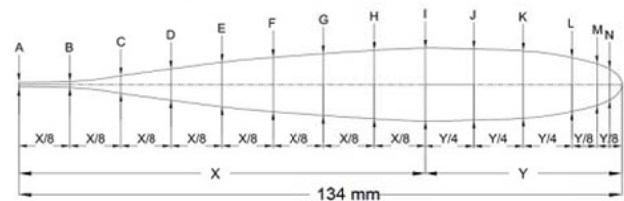


Figure 3: Airfoil profile of tail rotor blade.

### 2.3 Tests and Methods

To measure the aerodynamic characteristics, lift, drag and pitching-moment, the tail rotor blade was supported by a bracket that attach to force balance sensor. Figure 4 shows the schematic diagram of the tail rotor blade configuration in this experiment that mounted on force balance sensor via bracket support.

The type force balance sensor that's been used in this experiment is portable JR3 Force Balance, Figure 5. The balance has a capability to measure the aerodynamic forces and moment in 3-dimensional. The aerodynamic loads can be tested at various wind direction by rotating the model via the turntable. The accuracy of the balance is within 0.04% based on 1 standard deviation.

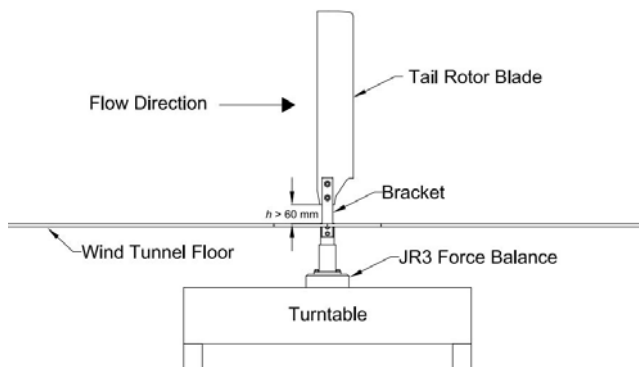


Figure 4: Schematic diagram of model-balance arrangement.

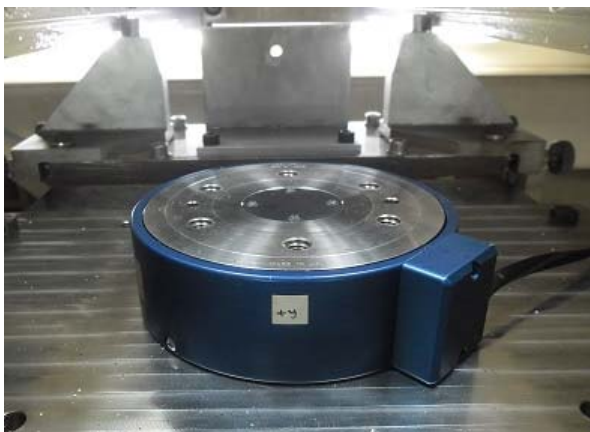


Figure 5: JR3 external force balance.

In this experiment, the wind tunnel speed was set from 5 m/s to 40 m/s, corresponds to a Reynolds number based on airfoil chord from  $0.419 \times 10^5$  to  $3.352 \times 10^5$  and angle of attack of 0, 5, 10, 12, 15, 18, 20, and 25 degrees. Since the blockage ratio is merely small, blockage corrections are assumed to be negligible.

Table 1 shows the set up air speed data from the wind tunnel.

Table 1: Wind tunnel air speed data

| Speed, V | Reynolds Number<br>(Re) $\times 10^{-5}$ | RPM   | Pressure,<br>mbar |
|----------|--|-------|-------------------|
| 5        | 0.419                                    | 54.0  | 14.7              |
| 10       | 0.838                                    | 103.5 | 59.1              |
| 15       | 1.257                                    | 152.5 | 133.2             |
| 20       | 1.676                                    | 200.5 | 235.5             |
| 25       | 2.095                                    | 249.0 | 368.8             |
| 30       | 2.514                                    | 297.0 | 530.8             |
| 35       | 2.933                                    | 345.0 | 721.8             |
| 40       | 3.352                                    | 393.0 | 945.4             |

In order minimize the sidewall boundary-layer interference effects on the balance measurements, the blade model was placed distance from the floor. The gap of 60 mm was provided between lowest parts blade model and upper surface wind tunnel floor to minimize airflow and provide clearance for balance measurement, Figure 4 and Figure 5 shown the gap in the between of the blade bracket that has been mounted with a force balance sensor which position under the wind tunnel floor.

The laminar-separation and turbulence-reattachment location were determined using the oil dot technique. The smoke test follows up after the oil dotted test already done. The objective this test is to visualize the flow pattern on the blade, before and after the stall angle happen to the blade. The typical result for this test is shown Figure 9.



Figure 6: Gap between tail rotor blades with wind tunnel floor.

### 3.0 AXIAL, NORMAL, LIFT, AND DRAG FORCE DIRECTIONS PROCEDURE

The force coefficient  $F_X$  and  $F_Y$  are parallel and perpendicular to the chord line of the blade, whereas the more usual coefficient  $F_L$

and  $F_D$  are defined with reference to the direction of the free-stream airflow. (E.L Houghton, 2013)

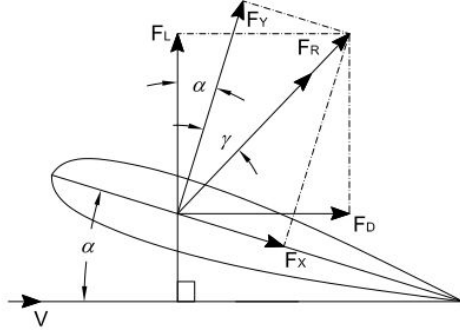


Figure 7: Definition: axial, normal, lift, and drag force directions.

The conversion from one pair of coefficient to the other may be carried out with reference to Figure 7 which is  $F_R$ , the coefficient of the resultant aerodynamic force, act at an angle  $\gamma$  to  $F_Y$ .  $F_R$  is the result both of  $F_X$  and  $F_Y$  and of  $F_L$  and  $F_D$ ; therefore, based on the Figure 7, it can be defined that

$$F_L = F_R \cos(\gamma + \alpha) = F_R \cos \gamma \cos \alpha - F_R \sin \gamma \sin \alpha \quad (1)$$

But  $F_R \cos \gamma = F_Y$  and  $F_R \sin \gamma = F_X$ , so

The lift force is defined by:

$$F_L = F_Y \cos \alpha - F_X \sin \alpha \quad (2)$$

Similarly, the drag force also defined by:

$$F_D = F_R \sin(\gamma + \alpha) = F_Y \sin \alpha + F_X \cos \alpha \quad (3)$$

And finally, the coefficients are given by the relationships

$$\text{Lift coefficient, } C_L = \frac{F_L}{\frac{1}{2} \rho V^2 S} \quad (4)$$

$$\text{Drag coefficient, } C_D = \frac{F_D}{\frac{1}{2} \rho V^2 S} \quad (5)$$

#### 4.0 RESULT AND DISCUSSION

The aerodynamic characteristics of the tail rotor blade were measured by using external balance system. As mentioned previously, the test wind speed was set from 5 m/s to 40m/s with increment 5 m/s for every test, and the blade setting angle of attack for this test is 0, 5, 10, 12, 15, 18, 20, and 25 degrees.

To correctly subtract the interface drag, the additional test with only bracket without tail rotor blades with similar condition such as air speed and angle of attack was executed.

Before starting the test, a tare reading was taken for every test with the wind off (where air speed is equal to 0 m/s) to get a measurement of the bias data.

Repeatability tests had also be conducted to ensure getting precise reading and validate the quality of measured results. Figure 8 depicts the sample reading in a time series data for angle

of attack 15 degrees and air speed set to 40 m/s from the external balance sensor.

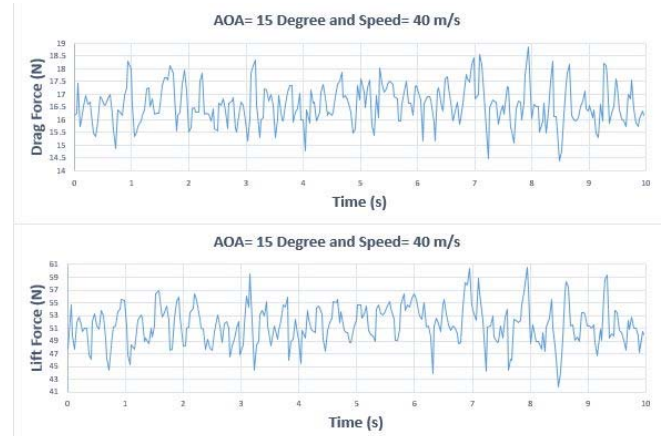


Figure 8: Time series data from external balance sensor.



Figure 9: Smoke test and oil dot test.

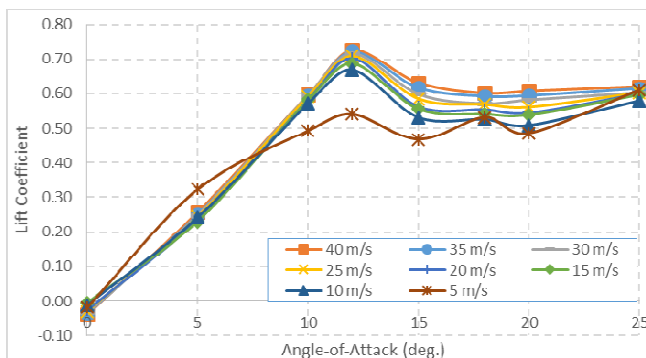


Figure 10: Lift coefficient versus angle of attack.

Graph in figure 10 shows the lift coefficient variations with different air test speed. At an angle of attack 12-13 degree shows the peak of lift coefficient where maximum lift happens before it drops after this points. And this condition is a critical or stalling angle of attack where the tail rotor blade starts to be less efficient to generate lift after beyond this angle of attack.

The reason the stall happens in the first place is because the air under heavier pressure beneath the blade finds it easier to creep forwards over the upper surface from the trailing edge as the angle against the relative airflow increases, because the upper air has started to slow down and now has an unfavorable pressure gradient, past the suction peak. It has longer to travel and more surface friction to cope with, so it doesn't have the energy to keep flowing and create the same pressure differential, and the amount of lift is reduced (the pressure at the trailing edge is atmospheric anyway). As the boundary layer has less momentum, it works harder keeping to surface (Phil Croucher, 2013).

Boundary layer separation is therefore produced from the adverse pressure gradient, when air start flowing in the reverse direction of the free stream, forcing itself under the normal airflow which has started to slow down. This flow we can see through the smoke and oil dot test like in Figure 9. This test will shows the patterns of airflow on the blade, before and after stalling angle happen.

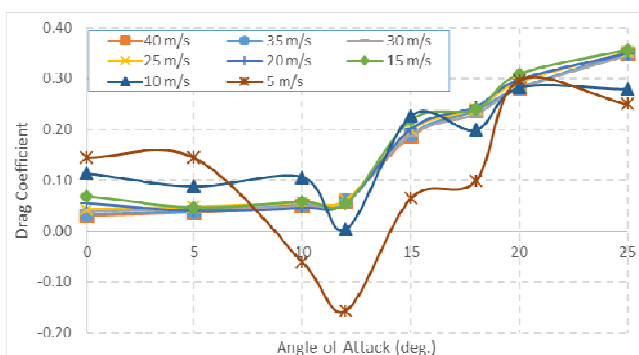


Figure 11: Drag coefficient versus angle of attack.

Although the lift force is still can be produced after that angle, the blade has a hard time to generate it. Stalling can alleviate by increasing the speed of airflow on the blade. But this will be lead to an increment of drag coefficient of tail rotor blades as shown in Figure 11. After the angle of attack 12-13 degrees, the drag coefficient rapidly increased, corresponds to an increment of angle of attack and speed of airflow. The coefficient of drag becomes steady after airflow speed achieved 15 m/s and above. However it is should be noted both Figure 10 and Figure 11 indicate bad readings for data taken at  $V=5$  m/s. This is because at a very low speed as 5 m/s, the flow is slightly fluctuated since UTM-LST is not built for the low speed flow experiment.

## 6.0 CONCLUSION

The general aerodynamics and performance characteristics of the full scaled generic model tail rotor blades of Agusta Bell 206B helicopter by experimental works have been obtained at speed 5 m/s to 40 m/s, corresponds to a Reynolds number based on airfoil chord from  $0.419 \times 10^5$  to  $3.352 \times 10^5$  in the UniversitiTeknologi Malaysia-Low Speed Tunnel (UTM-LST). The tests were conducted in a manner as to minimize both experimental apparatus and instrumentation uncertainties. Nevertheless it is conceded that there could be discrepancies with the exact data of the 206B rotor tail blade since some assumptions had been made, and due to limitations of experimental set-up during the wind tunnel testing.

## REFERENCE

1. Alias Mohd Noor and Shuhaimi Mansor. 2013. *Measuring Aerodynamic Characteristics Using High Performance Low Speed Wind Tunnel at Universiti Teknologi Malaysia*. Transport Research Alliance, Universiti Teknologi Malaysia.
2. E.L. Houghton, P.W. Carpenter, Steven Collicott and Dan Valentine. 2012. *Aerodynamics for Engineering Students (Sixth Edition)*. Butterworth-Heinemann. Page: 54-55.
3. Elfstrom GM. 2007. *History of Test Facility Design Expertise at Aiolos, Engineering Corporation*. AIAA 45th AIAA Aerospace Sciences Meeting and Exhibit, Reno, Nevada, USA.
4. Firdaus Mahamad, Jaswar Koto, M.S Ammoo and I.S.Ishak, 2014, Application of Quasi-Continuous Vortex Lattice Method to Determine Aerodynamic Characteristics of Helicopter Tail Rotor Propeller, *Proceeding of Ocean, Mechanical and Aerospace -Science and Engineering-, Vol.1, pp.44.52*, Pekanbaru, Indonesia.
5. Hao Rui, Jaswar Koto, 2014, *Prediction of Propeller Performance Using Quasi-Continuous Method*, Journal of Ocean, Mechanical and Aerospace -Science and Engineering-, Vol.10, pp.12-18.



6. Mohd. Shariff bin Ammoo, Ziad Bin Abdul Awal, Jaswar Koto, 2015, *Air Flow Characteristics and Behaviour of Main Rotor Blade of Remote Controlled Model Scale Helicopter*, Journal of Ocean, Mechanical and Aerospace - Science and Engineering-, Vol.16, pp.18-22.
7. Naoto Nakamura. 1985. *Estimation of Propeller Open-Water Characteristics Based on Quasi-Continuous Method*. Spring Meeting of The Society of Naval Architects of Japan. Japan.
8. Phil Croucher. 2013. *Private Helicopter Pilot Studies JaaBw*. Electrocuton (January 7, 2015).